



Predictive value of clinical and radiomic features for radiation therapy response in patients with lymph node-positive head and neck cancer

Ciro Franzese MD^{1,2} | Sara Lillo MD³  | Luca Cozzi PhD²  |
 Maria Ausilia Teriaca MD² | Marco Badalamenti MD² |
 Luciana Di Cristina MD^{1,2} | Veronica Vernier MD^{1,2} | Sara Stefanini MD^{1,2} |
 Damiano Dei MD^{1,2} | Stefano Pergolizzi MD³ | Armando De Virgilio MD^{1,4} |
 Giuseppe Mercante MD^{1,4} | Giuseppe Spriano MD^{1,4} | Pietro Mancosu PhD² |
 Stefano Tomatis MSc² | Marta Scorsetti MD^{1,2}

¹Department of Biomedical Sciences, Humanitas University, Pieve Emanuele, Italy

²Department of Radiotherapy and Radiosurgery, IRCCS Humanitas Research Hospital, Rozzano, Italy

³Department of Biomedical, Dental Science and Morphological and Functional Images, University of Messina, Messina, Italy

⁴Otorhinolaryngology Unit, IRCCS Humanitas Research Hospital, Rozzano, Italy

Correspondence

Luca Cozzi, Department of Radiotherapy and Radiosurgery, IRCCS Humanitas Research Hospital, Via Alessandro Manzoni 56, 20089 Rozzano (MI), Italy.
 Email: luca.cozzi@humanitas.it

Abstract

Background: Prediction of survival and radiation therapy response is challenging in head and neck cancer with metastatic lymph nodes (LNs). Here we developed novel radiomics- and clinical-based predictive models.

Methods: Volumes of interest of LNs were employed for radiomic features extraction. Radiomic and clinical features were investigated for their predictive value relatively to locoregional failure (LRF), progression-free survival (PFS), and overall survival (OS) and used to build multivariate models.

Results: Hundred and six subjects were suitable for final analysis. Univariate analysis identified two radiomic features significantly predictive for LRF, and five radiomic features plus two clinical features significantly predictive for both PFS and OS. The area under the curve of receiver operating characteristic curve combining clinical and radiomic predictors for PFS and OS resulted 0.71 (95%CI: 0.60–0.83) and 0.77 (95%CI: 0.64–0.89).

Conclusions: Radiomic and clinical features resulted to be independent predictive factors, but external independent validation is mandatory to support these findings.

KEYWORDS

head and neck cancer, predictive factor, predictive model, radiomics, radiotherapy

This is an open access article under the terms of the [Creative Commons Attribution-NonCommercial-NoDerivs](https://creativecommons.org/licenses/by-nc-nd/4.0/) License, which permits use and distribution in any medium, provided the original work is properly cited, the use is non-commercial and no modifications or adaptations are made.

© 2023 The Authors. *Head & Neck* published by Wiley Periodicals LLC.

1 | INTRODUCTION

Head and neck cancer (HNC) represents the sixth most common nonskin cancer worldwide, and in the United States there are about 600 000 incident cases of HNC annually.¹ In the European Union the estimated number of new annual HNC cases is about 107 000.²

Despite great advances have been made in the prevention and diagnosis over the past decades, the management of HNC still remains challenging when compared to tumors in other areas of the body because it strongly depends on pretreatment factors and prognosis. In addition, HNC covers a wide spectrum of heterogeneous diseases including tumors originating from the oral cavity, nasopharynx, oropharynx, hypopharynx, and larynx.

Currently, the standard of care for nonmetastatic locoregionally advanced HNC is surgery followed by postoperative radiotherapy (RT) or chemoradiotherapy (CRT) if indicated, or definitive CRT or induction chemotherapy followed by concomitant CRT for patients with unresectable HNC unfit for surgery or when organ preservation is one of the goals.³ However, great disparities exist in the treatment response.

Indeed, not all HNC have the same prognosis and subsets of patients may live for years or benefit from more aggressive therapies. Therefore, useful prognostic scores and omics technologies that help to predict survival, outcome, and treatment response are essential to guide personalized treatment decisions and properly stratify patients in future research.

Radiomics is the field of computational medicine that allows the extraction of features from standard biomedical imaging and generation of predictive models.⁴ Its potential applications are extensive, both for the interpretation of data resulting from modern imaging modalities and for the identification of new features undetectable through the human eyes, thus overcoming several limits of conventional imaging and fostering further advances in RT.^{4,5}

Radiomics and machine learning approaches have found several applications in the HNC field, such as the development of prognostic biomarkers,^{6–8} radiomics strategies for predicting tumor response,^{9–11} as well as the detection of HPV status in patients with oropharynx cancer.^{11,12} Furthermore, normal tissues radiomics information is likely to reflect potential risks for late radiation-induced toxicities.^{13,14} More recently, the nodal tumor burden is gaining increasing interest as cervical nodal metastasis are a well-known prognostic negative factor and advanced nodal stage is predictive for increased distant metastases and lower survival in HNC.^{15–18} A comprehensive overview of big data applications in the HNC field that should be taken into account in the decision-making process is provided by Resteghini et al.¹⁹

In light of this rapidly evolving scenario towards a tailored RT, the present study aims at developing radiomics- and clinical-based models able to predict survival and treatment response by employing computed tomography (CT) pretreatment imaging data of metastatic lymph nodes (LNs) and clinical variables of patients with HNC submitted to definitive RT/CRT.

2 | MATERIALS AND METHODS

2.1 | Patients and treatment

All the head and neck squamous cell carcinoma (HNSCC) patients with LNs treated between February 2016 and January 2022 were included in this retrospective single-institution analysis.

Inclusion criteria were histologically proven squamous cell carcinomas with metastatic LNs defined radiologically and/or by cytology, submitted to definitive RT/CRT, with an Eastern Cooperative Oncology Group (ECOG) performance status ≤ 2 and a minimum follow-up time of 6 months. Patients were excluded if surgery or irradiation was previously performed, if the disease was metastatic at onset or if metallic CT artifacts altered the radiological region of LNs.

TNM (tumor, node, and metastases) classification was scored according to the 8th Edition of the American Joint Committee on Cancer (AJCC) staging system and the HPV status of oropharyngeal cancer was assessed by immunohistochemical p16 staining in biopsy specimens.

All patients underwent contrast-free and contrast-enhanced pretreatment planning imaging of the head and neck according to the same scanning protocol with 120 kVp and 300 mAs on the same CT scanner (Brilliance Big Bore, Philips, Amsterdam, The Netherlands). CT images were acquired with 3 mm slice thickness and an in-plane resolution of 0.8 mm. In addition, other pretreatment or planning imaging modalities such as magnetic resonance imaging (MRI) and/or positron emission tomography-computed tomography (PET-CT) were acquired in almost all cases to better identify the LNs and primary tumors.

All treatments consisted of volumetric modulated arc therapy (VMAT) with 6 MV photon beams and the treatment planning and dose calculation were performed using the Eclipse planning system version 11 (Varian Medical Systems, Palo Alto, CA).

Depending on tumor origin and performance status, the prescription dose varied between three different simultaneous integrated boost regimens, respectively, to the high-risk and low-risk volumes: 66/54 Gy in 30 fractions, 69.96/54.45 Gy in 33 fractions, and 70/56 Gy in 35 fractions.

The entire anatomical neck levels to which the LNs belonged were incorporated in the high-risk treatment volume, whereas the low-risk nodal target volumes were defined according to Biau et al.²⁰ Consensus guidelines were used for the delineation of the primary tumor clinical target volumes.²¹

All patients were treated according to the Declaration of Helsinki and provided informed general consent both to the treatment and the scientific use of their clinical data.

Follow-up was performed with clinical examination plus MRI or CT at 2 months and PET-CT at 12 weeks after the treatment conclusion. Then clinical-radiological follow-up according to physician's discretion occurred every 3 months for the first 3 years, every 6 months for the following 2 years, and then annually thereafter.

2.2 | Radiomics analysis

The contrast-free and postcontrast planning CT were loaded into the Eclipse planning system and geometrically aligned with the pretreatment MRI and/or PET-CT, if available. All LNs were individually manually segmented by two expert radiation oncologists on axial slices of the contrast-free planning CT. The DICOM files of the volumes of interest (VOI) thus obtained were finally uploaded on LIFEx v7.0 for feature extraction.

First, input parameters were defined. Spatial resampling to $1.2 \times 1.2 \times 3$ mm and an absolute intensity rescaling with a minimum bound of -1000 and a maximum bound of 3000 were performed. The number of gray levels was set to 400 with a bin size of 10 .

A total of 39 features was extracted for each patient. The first-order features consisted of shape and histogram features. The second order features included the gray level co-occurrence matrix (GLCM), the neighborhood gray level different matrix (NGLDM), the gray level run length matrix (GLRLM), and the gray level zone length matrix (GLZLM).

2.3 | Statistical analysis

All the radiomic features as well as the clinical features such as age, sex, smoking status, TNM stage, chemotherapy administration, and performance status were simultaneously investigated for their predictive value relatively to locoregional failure (LRF), progression-free survival (PFS), and overall survival (OS) with univariate Cox regression.

Optimal separation thresholds were determined per each predictor by identifying the lowest p -value in the p -value distribution from the Wilcoxon test, provided that each group contained a number of patients greater than

or equal to 15 , which approximately corresponds to the 15% of the entire sample.

Then a minimal set of significant features was obtained by means of elastic net regularization, which is a process that is able to automatically select the most significant independent covariates from a group of multiple cross-related variables.

Briefly, aimed at identifying potential results redundancy, the mutual correlation between features was evaluated for the best performing covariates ($p \leq 0.05$). Covariates showing Pearson correlation values with $p \geq 0.05$ were considered not cross-related and used for further analyses.

Multivariate Cox regression was then performed including in the model only the uncorrelated features resulting from the elastic net regularization, and only the variables surviving after a backward elimination phase were considered to have a predictive value relatively to LRF, PFS, and OS.

Calibration was evaluated with Hosmer and Lemeshow test. The data of the whole dataset were split into low- (below threshold) and high-risk (above threshold) groups by the median of the Cox's prediction, similarly to Aerts et al.²²

Performance of multivariate models was evaluated with the area under curve (AUC) of receiver operating characteristic (ROC) curve. The standard ROC curve was computed by testing the sensitivity and specificity of the models in predicting the outcome from the selected predictors of the model.

The statistical analysis of the data was performed through the open source R platform (version 3.6).

3 | RESULTS

Overall 106 subjects treated from February 2016 to January 2022 were suitable for final analysis and the whole dataset was used for training creating a Transparent Reporting of a multivariable prediction model for Individual Prognosis Or Diagnosis (TRIPOD) type 1a model.²³

The clinical and demographic characteristics, as well as the treatment parameters, are summarized in Table 1. Exclusive concomitant CRT was delivered in $80/106$ patients, induction chemotherapy followed by concomitant CRT was administered in $15/106$ patients, whereas the remaining $11/106$ patients were submitted to RT alone.

Table 2 provides the median and mean time for LRF, PFS, and OS of the entire cohort.

3.1 | Locoregional failure

The univariate Cox regression analysis identified five significant features for LRF, but after elastic net

TABLE 1 Patients' clinical and demographics information

Number of patients	106
Sex	Male: 77 (73%) Female: 29 (27%)
Age, years ^a	63 (35–83)
ECOG performance status	0: 71 (67%) 1: 27 (26%) 2: 8 (7%)
Smoking status	Smokers: 44 (42%) Nonsmokers: 34 (32%) Ex-smokers: 28 (26%)
Site	Oropharynx: 68 (65%) Nasopharynx: 11 (10%) Hypopharynx: 11 (10%) Larynx: 11 (10%) Oral cavity: 5 (5%)
HPV-positive status	40 (38%)
TNM stage	I: 5 (5%) II: 10 (9%) III: 31 (29%) IVA: 48 (46%) IVB: 12 (11%) T1-2: 44 (41.5%) T3-4: 62 (58.5%) N1: 28 (26.4%) N2: 68 (64.2%) N3: 10 (9.4%)
Chemotherapy	Induction TPF: 15 (14%) Concomitant: 95 (89.6%) 3-weekly cisplatin: 72 (67.9%) Weekly cisplatin: 6 (5.7%) Cetuximab: 17 (16.0%) No: 11 (10%)
Prescription dose	66/54 Gy in 30 fractions: 102 (96%) 69.96/54.45 Gy in 33 fractions: 2 (2%) 70/56 Gy in 35 fractions: 2 (2%)
Overall treatment time, days ^a	43 (39–69)
Median follow-up, months ^a	18.5 (6–74)

^aMedian and range in parentheses.

regularization and elimination of correlated features only two features remained significant (GLZLM_SIZE and GLZLM_SZHGE). Figure 1 illustrates the LRF graphs stratified according to the two significant predictors.

TABLE 2 Median and mean time ± standard deviation in months for locoregional failure, progression-free survival, and overall survival

Locoregional failure (months)	
Median	16.62
Mean ± standard deviation	26.42 ± 21.10
Progression-free survival (months)	
Median	15.58
Mean ± standard deviation	25.28 ± 21.55
Overall survival (months)	
Median	23.12
Mean ± standard deviation	29.25 ± 21.24

The AUC from the ROC curve built out of the model resulted 0.56 (95% confidence interval (95%CI): 0.43–0.69).

Figure 1 shows the AUC-ROC curve as well as the multivariate Cox model built for the LRF. In the survival curves, solid blue lines represent the low-risk group of patients, whereas dashed blue lines correspond to the high-risk group. The *p*-value from the Wilcoxon test comparison between low- and high-risk groups resulted 0.735.

3.2 | Progression-free survival

As regards the PFS and OS, we found the same significant clinical-radiomic signature. In particular, 13 radiomics predictors resulted significant at univariate analysis. However, elastic net regularization led to five significant predictors (GLCM_Entropy_log10, GLCM_Correlation, GLZLM_LGZE, Skewness, Kurtosis). Performance status and concomitant CRT were significant clinical predictors with a *p*-value of 0.03 for both of them.

The AUC from the ROC curve built out of the model using only clinical predictors for PFS resulted 0.58 (95%CI: 0.51–0.65). The *p*-value from the Wilcoxon test comparison between low- and high-risk groups resulted 0.005.

When considering only radiomic features, the AUC from the ROC curve built out of the model for the PFS resulted 0.62 (95%CI: 0.50–0.73). The *p*-value from the Wilcoxon test comparison between low- and high-risk groups resulted 0.025.

Finally, the AUC from the ROC curve combining clinical and radiomic predictors for PFS resulted 0.71 (95%CI: 0.60–0.83), thus outperforming the models based only on either clinical or radiomic predictors.

Figure 2 shows the AUC-ROC curve as well as the multivariate Cox model built for the PFS combining clinical and radiomic predictors. In the survival curves, solid

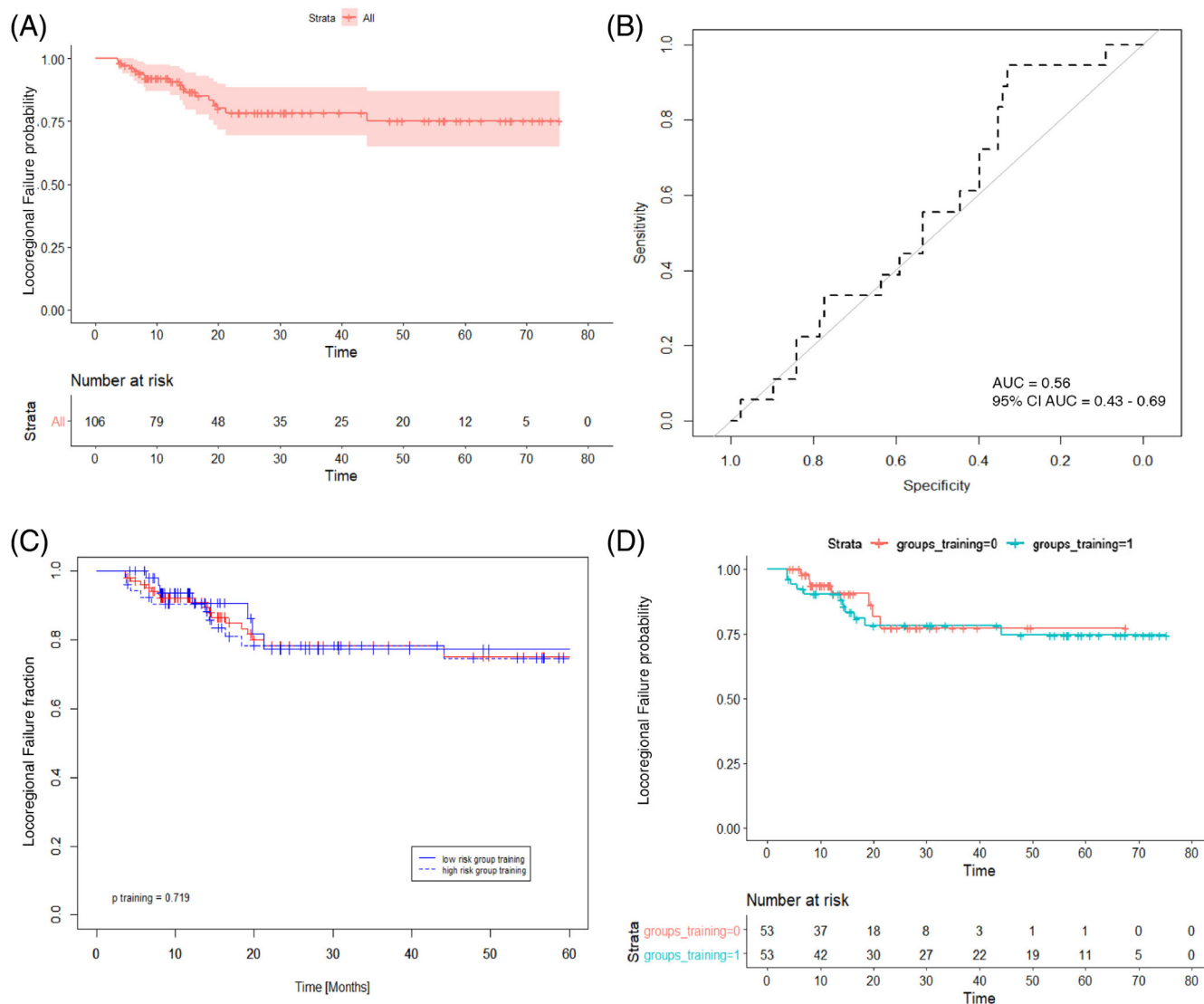


FIGURE 1 (A) Locoregional failure (LRF) curve for the entire dataset without any stratification. (B) The area under the curve (AUC) from the receiver operating characteristics (ROC) curve built out of the model for LRF. (C) LRF curves for the multivariate model; solid blue lines represent the low-risk group of patients, dashed blue lines correspond to the high-risk group, solid red line represents the entire patient cohort. (D) LRF curves with number of subjects at risk for the high- (blue) and low-risk (red) groups [Color figure can be viewed at wileyonlinelibrary.com]

blue lines represent the low-risk group of patients, whereas dashed blue lines correspond to the high-risk group. The p -value from the Wilcoxon test comparison between low- and high-risk groups resulted 0.

3.3 | Overall survival

Concerning the OS, the AUC from the ROC curve built out of the model using only clinical predictors resulted 0.71 (95%CI: 0.59–0.83). The p -value from the Wilcoxon test comparison between low- and high-risk groups resulted 0.003.

The AUC from the ROC curve built out of the model using only radiomic predictors for the OS resulted 0.61 (95%CI: 0.49–0.72). The p -value from the Wilcoxon test comparison between low- and high-risk groups resulted 0.098.

Finally, the AUC from the ROC curve combining clinical and radiomic predictors for OS resulted 0.77 (95% CI: 0.64–0.89), thus outperforming the models based only on either clinical or radiomic predictors.

Figure 3 shows the AUC-ROC curve as well as the multivariate Cox model built for the OS combining clinical and radiomic predictors. In the survival curves, solid blue lines represent the low-risk group of patients,

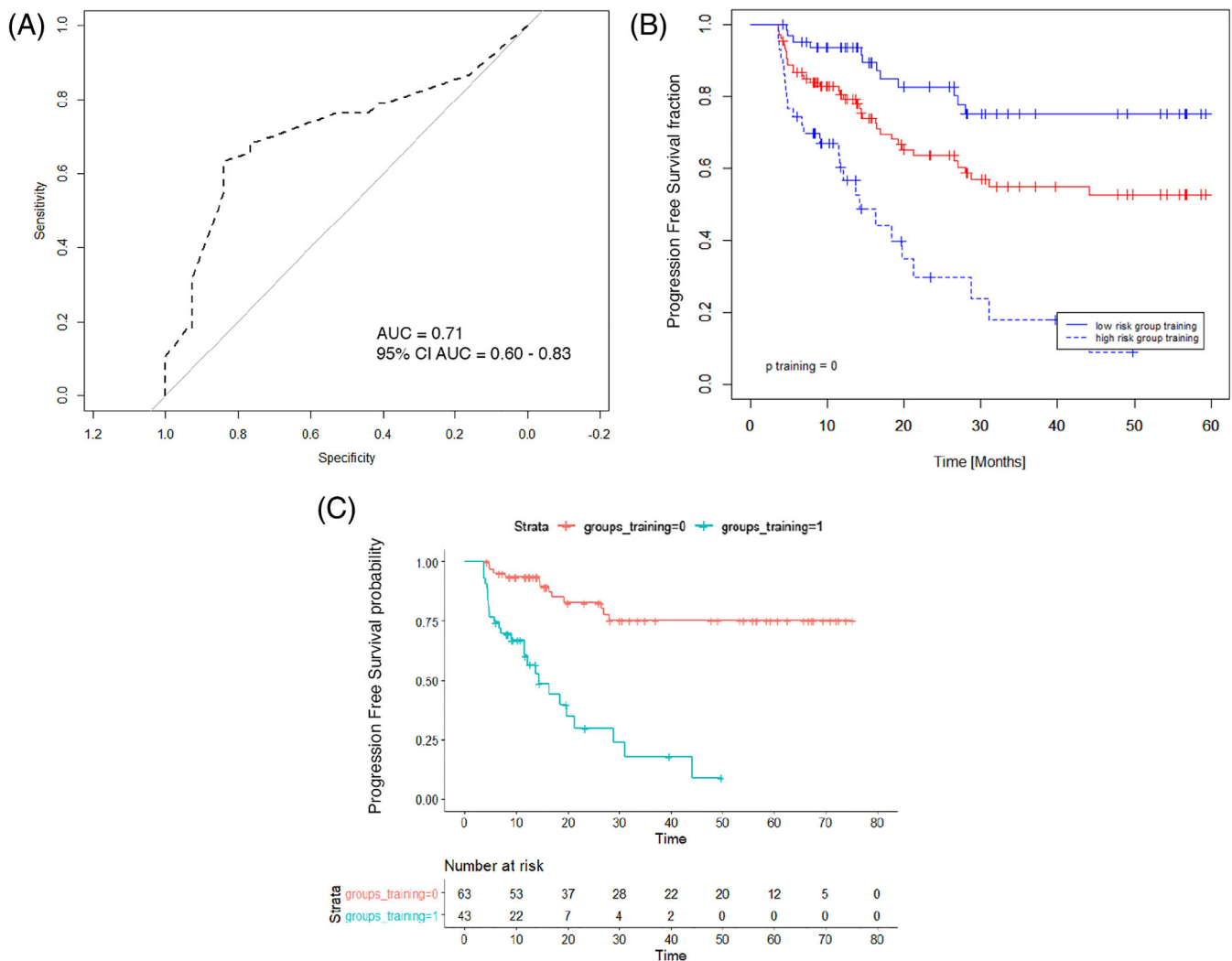


FIGURE 2 (A) The area under the curve (AUC) from the receiver operating characteristics (ROC) curve built out of the model combining clinical and radiomic predictors for progression-free survival (PFS). (B) PFS curves for the multivariate combined model built; solid blue lines represent the low-risk group of patients, dashed blue lines correspond to the high-risk group, solid red line represents the entire patient cohort. (C) PFS curves with number of subjects at risk for the high- (blue) and low-risk (red) groups [Color figure can be viewed at wileyonlinelibrary.com]

whereas dashed blue lines correspond to the high-risk group. The p -value from the Wilcoxon test comparison between low- and high-risk groups resulted 0.001.

A list of the clinical and radiomics features found to be significant at the univariate analysis can be found in Table 3.

4 | DISCUSSION

To the best of our knowledge, this is the first study investigating in HNSCC submitted to definitive RT/CRT possible CT-based radiomics signatures extracted by positive nodes imaging data that correlate significantly with LRF, PFS, and OS. Indeed, up so far, LNs radiomic features

have been used only to develop and validate a pretreatment prediction model for nodal failure.¹⁷ In particular, multivariable analysis disclosed three clinical features (T-stage, sex, and PS) and two radiomic features (Least-axis-length representing nodal size and GLCM_Correlation) as independent prognostic factors of lymph node failure in HNSCC. Interestingly, such a combined model outperformed the models based either on clinical features or radiomics alone in terms of discrimination.

Herein, we found that CRT and PS as clinical features and skewness, kurtosis, entropy, GLCM_Correlation, and GLZLM_LGZE as radiomic features were independent predictor factors of PFS and OS, especially when using the combined clinical-radiomics model. It is worth to note that the clinical feature PS and the radiomic feature

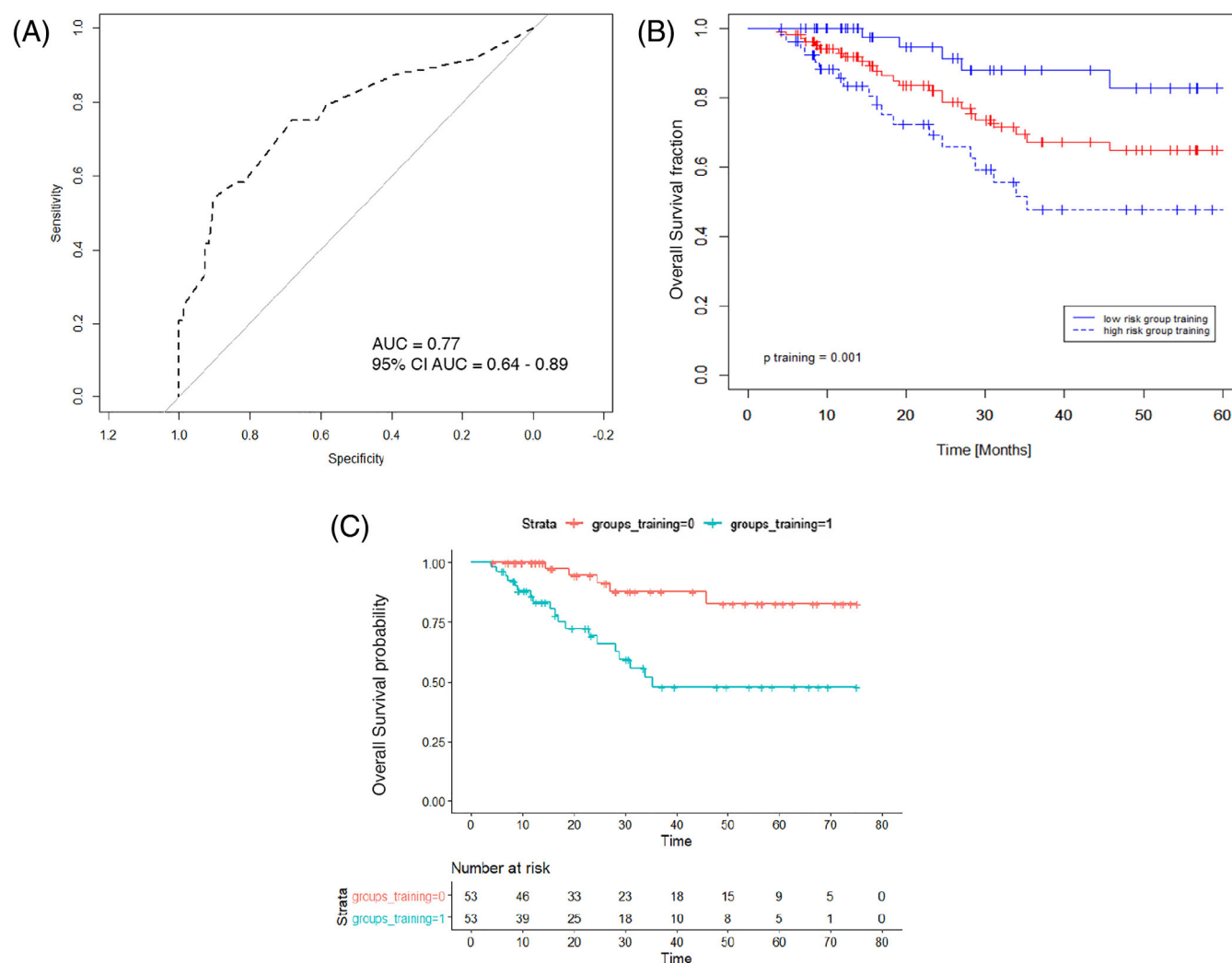


FIGURE 3 (A) The area under the curve (AUC) from the receiver operating characteristics (ROC) curve built out of the model combining clinical and radiomic predictors for overall survival (OS). (B) OS curves for the multivariate combined model built; solid blue lines represent the low-risk group of patients, dashed blue lines correspond to the high-risk group, solid red line represents the entire patient cohort. (C) OS curves with number of subjects at risk for the high- (blue) and low-risk (red) groups [Color figure can be viewed at wileyonlinelibrary.com]

GLCM_Correlation are consistent with the results of previous studies evaluating the potential of radiomics prediction in HNSCC.^{17,24,25}

Despite only two radiomics features resulted to be predictive for LRF, interestingly the same clinical and radiomic signature resulted to be significantly predictive for PFS and OS, thus increasing the robustness of their predictability.

Explaining why some features are significant rather than others and their meanings still remains a challenging task, though previous evidence suggested that the radiomics signatures identified are strongly affected by tissue homogeneity. For instance, skewness and kurtosis reflect the asymmetry and the shape of the gray-level

distribution, respectively, whereas GLCM_Correlation is a textural feature describing the correlation of a reference voxel to its neighbors. Altogether, these results may suggest intranodal heterogeneity, which is likely to result by the coexistence of multiple subclonal populations within the LNs, as a significant noninvasive imaging-based predictor for PFS and OS.

The relevance of tissue homogeneity in predicting PFS after CRT in locally advanced HNSCC has been also recently demonstrated by Cozzi et al. by means of CT-based radiomic analysis on the primary tumor.²⁶ In particular, their model including Shape_Compacity and GLCM_Correlation was predictive for the PFS with a concordance index of 0.72 and 0.80 for the training and

TABLE 3 Clinical and radiomics features significant at the univariate analysis

Feature name	Threshold	p-value
Locoregional failure		
GLZLM_SZE	3.06	0.04
GLZLM_SZHGE	3.02	0.04
Progression-free survival/overall survival		
Performance status	0–2	0.03
Concomitant chemotherapy	0/1	0.03
Skewness	1.07	0.02
Kurtosis	1.13	0.02
Entropy (log ₁₀)	1.16	0.03
GLCM_Correlation	1.16	0.03
GLZLM_LGZE	1	0.02

validation dataset, respectively. In addition, while no clinical- or treatment-related feature could be identified as a predictive factor, only the use of induction chemotherapy approached significance in the analysis of PFS, despite not passing the selection criteria to be included in the model.

Several studies have attempted to identify, at the radiomic level, imaging characteristics that could discriminate between different treatment responses in HNC, though consistent and robust features have not yet emerged. This has made the application of radiomics in the clinical scenario limited, and the reasons for such a discrepancy between research studies and clinical practice are manifold. First, most radiomics studies have built their models from limited data, assuming to be representative of all other data for different institutions. Second, most research studies lack of validation of their generated models.

Several limitations exist also in the present study. First of all, it is a small cohort of patients from a single institution with very few events in the dataset that did not allow to separate it into training and testing subgroups, thus affecting both robustness and reproducibility of the results.

Furthermore, the lack of a radiomic dedicated standardized segmentation may underestimate or overestimate the true LNs volume. Indeed, the contouring process has a strong impact on the performance of the models being the first source of error in the complex process of radiomics analysis.²⁷

As regards features extraction, input parameters such as spatial resampling and absolute intensity rescaling methods were arbitrary. In addition, we decided to extract a small number of basic features excluding many higher order classes of features thus not investigating

their impact on prognosis and treatment response. Although this approach may appear simplistic, the underlying assumption is that, in order to improve our understanding on the hidden meaning of radiological data, it is advisable to begin from the most simple and reproducible features that might play a role in everyday clinical practice.

In addition, the predictive models here presented should be validated in a large independent external cohort in order to conduct a more valuable TRIPOD type 3 study, but it should be kept in mind that some technical aspects such as CT acquisition parameters could influence the reproducibility of our radiomics analysis.

Finally, though the use of noncontrast enhanced treatment planning CT datasets makes this kind of analyses potentially available to all patients scheduled for RT, LNs radiomic features from other imaging modalities such as MRI, PET-CT, and ultrasound could be investigated to further improve the current models' prediction for LRF, PFS, and OS.

It is worth to note that a simple and easily reproducible methodology was applied in the present retrospective study. However, as no gold standard currently exists for the development of clinical- and radiomics-based predictive models, different approaches should be tested and critically compared. Hence, further studies are then warranted to obtain a multimodal-imaging radiomic patient characterization and develop reliable radiological-based diagnostic and therapeutic markers for HNC.

5 | CONCLUSIONS

Metastatic lymph nodes CT-based radiomic signatures and clinical features resulted to be independent predictor factors of PFS, LRF, and OS in patients with HNC submitted to definitive radiotherapy with or without chemotherapy. Further validation studies on larger, prospective and multicenter cohorts are mandatory to confirm these findings and to improve the predictive models and clinical strategies currently employed.

ACKNOWLEDGMENT

Open access funding provided by BIBLIOSAN.

CONFLICT OF INTEREST STATEMENT

Luca Cozzi acts as scientific advisor to Varian Medical Systems and is a clinical research scientist at Humanitas Research Hospital. Ciro Franzese, Sara Lillo, Maria Ausilia Teriaca, Marco Badalamenti, Luciana Di Cristina, Veronica Vernier, Sara Stefanini, Damiano Dei, Stefano Pergolizzi, Armando De Virgilio, Giuseppe Mercante,

Giuseppe Spriano, Pietro Mancosu, Stefano Tomatis, and Marta Scorsetti declare that they have no competing interests.

DATA AVAILABILITY STATEMENT

Data are available on request due to privacy/ethical restrictions.

ETHICS STATEMENT

The Ethics Committee approved by notification this retrospective study. All patients provided consent for retrospective studies at hospital admission.

ORCID

Sara Lillo  <https://orcid.org/0000-0001-7300-1168>

Luca Cozzi  <https://orcid.org/0000-0001-7862-898X>

REFERENCES

- Siegel RL, Miller KD, Jemal A. Cancer statistics, 2018. *CA Cancer J Clin.* 2018;68:7-30.
- Dyba T, Randi G, Bray F, et al. The European cancer burden in 2020: incidence and mortality estimates for 40 countries and 25 major cancers. *Eur J Cancer.* 2021;157:308-347.
- Machiels J-P, René Leemans C, Golusinski W, et al. Squamous cell carcinoma of the oral cavity, larynx, oropharynx and hypopharynx: EHNS-ESMO-ESTRO clinical practice guidelines for diagnosis, treatment and follow-up. *Ann Oncol.* 2020;31:1462-1475.
- Bibault JE, Xing L, Giraud P, et al. Radiomics: a primer for the radiation oncologist. *Cancer/Radiothérapie.* 2020;24:403-410.
- Boldrini L, Bibault JE, Masciocchi C, Shen Y, Bittner MI. Deep learning: a review for the radiation oncologist. *Front Oncol.* 2019;9:977.
- Parmar C, Grossmann P, Rietveld D, Rietbergen MM, Lambin P, Aerts HJWL. Radiomic machine-learning classifiers for prognostic biomarkers of head and neck cancer. *Front Oncol.* 2015;5:272.
- Parmar C, Leijenaar RTH, Grossmann P, et al. Radiomic feature clusters and prognostic signatures specific for lung and head & neck cancer. *Sci Rep.* 2015;5:11044.
- Zhai T-T, van Dijk LV, Huang B-T, et al. Improving the prediction of overall survival for head and neck cancer patients using image biomarkers in combination with clinical parameters. *Radiother Oncol.* 2017;124:256-262.
- Vallièrès M, Kay-Rivest E, Perrin LJ, et al. Radiomics strategies for risk assessment of tumour failure in head-and-neck cancer. *Sci Rep.* 2017;7:10117.
- Kaźmierska J, Kaźmierski MR, Bajon T, et al. Prediction of incomplete response of primary tumour based on clinical and radiomics features in inoperable head and neck cancers after definitive treatment. *J Pers Med.* 2022;12:1092.
- Bogowicz M, Riesterer O, Ikenberg K, et al. Computed tomography radiomics predicts HPV status and local tumor control after definitive radiochemotherapy in head and neck squamous cell carcinoma. *Int J Radiat Oncol Biol Phys.* 2017;99:921-928.
- Ranjbar S, Ning S, Zwart CM, et al. Computed tomography-based texture analysis to determine human papillomavirus status of oropharyngeal squamous cell carcinoma. *J Comput Assist Tomogr.* 2018;42:299-305.
- Abdollahi H, Mostafaei S, Cheraghi S, Shiri I, Rabi Mahdavi S, Kazemnejad A. Cochlea CT radiomics predicts chemoradiotherapy induced sensorineural hearing loss in head and neck cancer patients: a machine learning and multi-variable modelling study. *Phys Med.* 2018;45:192-197.
- Carbonara R, Bonomo P, Di Rito A, et al. Investigation of radiation-induced toxicity in head and neck cancer patients through radiomics and machine learning: a systematic review. *J Oncol.* 2021;2021:5566508.
- Magnano M, Bongioannini G, Lerda W, et al. Lymphnode metastasis in head and neck squamous cells carcinoma: multi-variate analysis of prognostic variables. *J Exp Clin Cancer Res.* 1999;18:79-83.
- Brockstein B, Haraf DJ, Rademaker AW, et al. Patterns of failure, prognostic factors and survival in locoregionally advanced head and neck cancer treated with concomitant chemoradiotherapy: a 9-year, 337-patient, multi-institutional experience. *Ann Oncol.* 2004;15:1179-1186.
- Zhai T-T, Langendijk JA, van Dijk LV, et al. Pre-treatment radiomic features predict individual lymph node failure for head and neck cancer patients. *Radiother Oncol.* 2020;146:58-65.
- Zhai T-T, Wesseling F, Langendijk JA, et al. External validation of nodal failure prediction models including radiomics in head and neck cancer. *Oral Oncol.* 2021;112:105083.
- Resteghini C, Trama A, Borgonovi E, et al. Big data in head and neck cancer. *Curr Treat Options Oncol.* 2018;19:62.
- Biau J, Lapeyre M, Troussier I, et al. Selection of lymph node target volumes for definitive head and neck radiation therapy: a 2019 update. *Radiother Oncol.* 2019;134:1-9.
- Grégoire V, Evans M, Le Q-T, et al. Delineation of the primary tumour clinical target volumes (CTV-P) in laryngeal, hypopharyngeal, oropharyngeal and oral cavity squamous cell carcinoma: AIRO, CACA, DAHANCA, EORTC, GEORCC, GORTEC, HKNPCSG, HNCIG, IAG-KHT, LPRHHT, NCIC CTG, NCRI, NRG Oncology, PHNS, SBRT, SOMERA, SRO, SSHNO, TROG consensus guidelines. *Radiother Oncol.* 2018;126:3-24.
- Aerts HJWL, Velazquez ER, Leijenaar RTH, et al. Decoding tumour phenotype by noninvasive imaging using a quantitative radiomics approach. *Nat Commun.* 2014;5:4006.
- Collins GS, Reitsma JB, Altman DG, Moons KGM. Transparent reporting of a multivariable prediction model for individual prognosis or diagnosis (TRIPOD): the TRIPOD statement. *BMJ.* 2015;350:g7594.
- van den Brekel MWM, Bindels EMJ, Balm AJM. Prognostic factors in head and neck cancer. *Eur J Cancer.* 2002;38:1041-1043.
- Zhai T-T, Langendijk JA, van Dijk LV, et al. The prognostic value of CT-based image-biomarkers for head and neck cancer patients treated with definitive (chemo-)radiation. *Oral Oncol.* 2019;95:178-186.
- Cozzi L, Franzese C, Fogliata A, et al. Predicting survival and local control after radiochemotherapy in locally advanced head and neck cancer by means of computed tomography based radiomics. *Strahlenther Onkol.* 2019;195:805-818.

27. Fontaine P, Andrearczyk V, Oreiller V, et al. Cleaning radiotherapy contours for radiomics studies, is it worth it? A head and neck cancer study. *Clin Transl Radiat Oncol*. 2022;33:153-158.

SUPPORTING INFORMATION

Additional supporting information can be found online in the Supporting Information section at the end of this article.

How to cite this article: Franzese C, Lillo S, Cozzi L, et al. Predictive value of clinical and radiomic features for radiation therapy response in patients with lymph node-positive head and neck cancer. *Head & Neck*. 2023;45(5):1184-1193. doi:[10.1002/hed.27332](https://doi.org/10.1002/hed.27332)